

The creep mechanism of ceramic matrix composites at low temperature and stress, by a material science approach

J.L. Chermant^{a,*}, G. Boitier^b, S. Darzens^a, G. Farizy^a,
J. Vicens^a, J.C. Sangleboeuf^c

^a*LERMAT, URA CNRS 1317, ISMRA, 6 Bd Maréchal Juin, 14050 Caen Cedex, France*

^b*DCI, ISMRA, 6 Bd Maréchal Juin, 14050 Caen Cedex, France*

^c*LARMAUR, UPRES JE 2310, Bât. 10B, Université de Rennes 1, Campus de Beaulieu, 35042 Rennes Cedex, France*

Received 7 October 2001; received in revised form 10 February 2002; accepted 28 February 2002

Abstract

This paper deals with the creep mechanism for ceramic matrix composites reinforced by long ceramic fibers in a ceramic or glass-ceramic matrix, tested at low stresses (<400 MPa) and low temperatures, respectively <1673 K for the former and <1373 K for the latter. The macroscopic results give few ideas on the mechanism, but observations at different scales until high resolution evidence brittle damages which lead the authors to use the damage mechanics approach and to demonstrate that a damage creep mechanism is operating for these CMCs in two steps: (1) matrix microcrack development until its saturation, (2) followed by the opening of some of these microcracks enabling under certain conditions creep of the SiC fibers which bridge the microcracks. This was enlightened by precise damage observations on stepping creep tests and by their quantification with automatic image analysis. © 2002 Elsevier Science Ltd. All rights reserved.

Keywords: Composites (ceramic matrix composites); Creep; Fibres; Damage; Electron microscopies

1. Introduction

Over the past 15–20 years, ceramic matrix composites reinforced by continuous ceramic fibers, CMCs, have been developed and tested in many aerospace and military turbine engines, and in some nuclear or ballistic applications.^{1–14} One can quote for example, combustor liners, exhaust vanes, exit cones, flame holders, hot gas valves, nozzle petals, thermal structural panels for space, thrust combustion chambers, transition liners, turbine nozzles and wheels. If these composites are considered as a class of high-tech materials for hot structural applications, over the last 10 years they are used not only in brake disks for aircrafts but also for race cars and motorcycles. In few years they are expected to be used for high speed trains, trucks and top

(first) class cars.^{15–18} These applications benefit from the low density, high strength, high chemical resistance to severe environment, un-brittle behavior, low emission and noise, ... of these CMCs in a field where unprotected metals or metallic alloys could not be used.

To develop new parts of CMCs or of any other material, the design bureau needs toughness and statistical data, and also life time parameters to accede to correct predictions under stress, creep and fatigue solicitations. Moreover to avoid a catastrophic rupture, the characteristics of the fiber/matrix interfaces or interphases must be based on an interphase to favour some specific microcrack deviations, generally in mode II, along the interfaces or within the interphases.^{19,20}

The aim of this paper is, mainly from the results on different creep investigations performed in our laboratory, to present the mechanism which governs the creep of ceramic matrix composites reinforced by long ceramic fibers (C_f and SiC_f) in a ceramic matrix (SiC and SiBC) or a glass-ceramic matrix (MLAS and YMAS). These composites were tested under stresses lower than

* Corresponding author. Tel.: +33-231-452-664; fax: +33-231-452-660.

E-mail address: jean-louischermant@ismra.fr (J.L. Chermant).

400 MPa and at temperatures lower than 1673 K for CMCs with a ceramic matrix and 1373 K for those with a glass-ceramic matrix. These experimental conditions were required to find a correct creep-mechanism indicator. This paper will focus more particularly on CMCs with a ceramic matrix.

2. Experimental

2.1. Materials

Many ceramic matrix composites with either a monolithic ceramic matrix or a glass-ceramic matrix were investigated in our laboratory: SiC_f -MLAS,^{21,22} SiC_f -YMAS²³ (with A=Al, L=Li, M=Mg, Y=Y, S=SiO₂), and C_f -SiC,²⁴ SiC_f -SiC^{25,26} and SiC_f -SiBC^{27,28}

All the CMCs with a monolithic ceramic matrix—2.5D C_f -SiC, 2D SiC_f -SiC and 2.5D SiC_f -SiBC—were fabricated by SEP-SNECMA (now SNECMA Propulsion Solide, Saint-Médard en Jalles, France) by a more or less complex chemical vapor infiltration (CVI) process.^{29,30} A thin layer of pyrolytic carbon was deposited on all the fiber performs (NLM 202 and Hi-Nicalon SiC_f fibers or ex PAN C_f fibers). SiC_f -SiBC composites are made of self sealing multilayered matrix based on Si-B-C phases. Three different batches of SiC_f -SiBC were investigated: N1 and N2 with NLM 202 SiC_f ,

which differ in the pyrocarbon interphase thickness and layer sequence, and H3 with high Nicalon (Hi-Nic) SiC_f . No more information can be given on these phases, due to confidentiality. The morphology and the microstructure of SiC_f -SiBC composites have previously been described by Darzens.^{27,31} Due to the difference in the thermal expansion coefficients between carbon and silicon carbide, C_f -SiC composites present some matrix microcracks in the as-received state, due to their fabrication process, which is not the case for SiC_f -SiC and SiC_f -SiBC composites.

CMCs with a glass-ceramic matrix—1D and (0–90°)₆ SiC_f -MLAS and 1D SiC_f -YMAS—were fabricated from a slurry of the adequate glass powders which embedded Nicalon NLM 202 SiC_f plies and then hot-pressed, by Aérospatiale (now EADS, Saint-Médard en Jalles, France) for 1D and 2D SiC_f -MLAS composites^{21,22} and by ONERA (Etablissement of Palaiseau, France) for 1D SiC_f -YMAS²³ composites.

Fig. 1 presents some micrographs of these materials.

2.2. Experimental procedures

C_f -SiC, SiC_f -SiC and SiC_f -SiBC composites were creep tested with a Schenck Hydropuls PSB 100 servo-hydraulic machine (Darmstadt, Germany), generally under a partial pressure of argon, between 1273 and 1673 K at a stress up to 250 MPa. Some tests were also performed in air for SiC_f -SiBC. This machine was

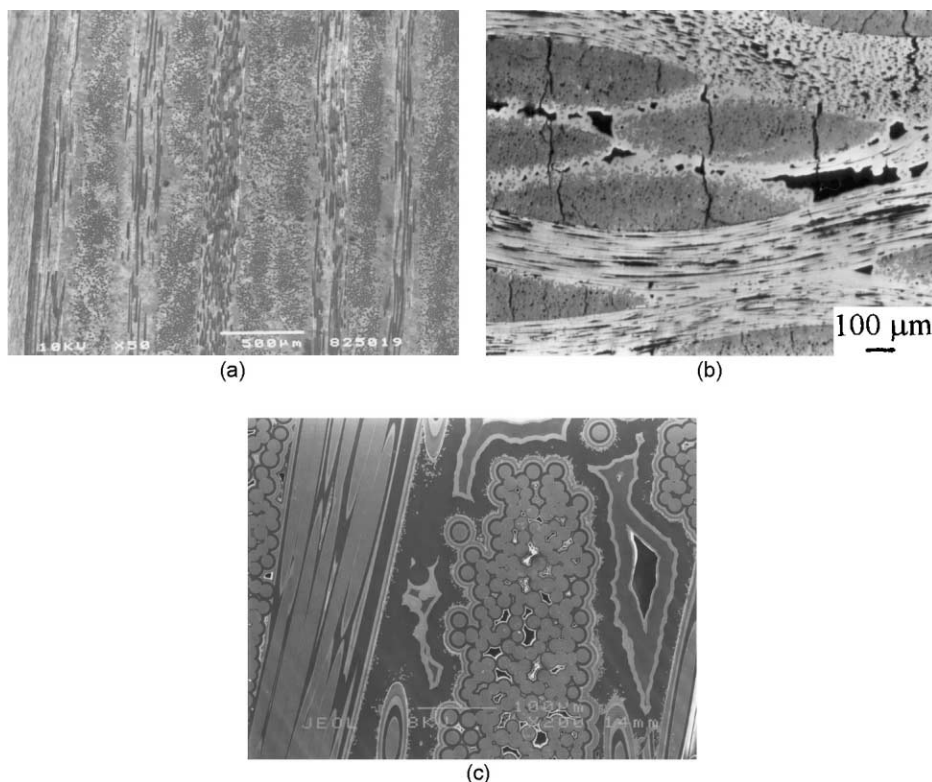


Fig. 1. SEM micrographs of a (0–90°)₆ SiC_f -MLAS (a), 2.5D C_f -SiC (b) and SiC_f -SiBC (c).

equipped with an airtight fence and an induction furnace (AET and Célès, respectively Meylan and Lautenbach, France). Strain was measured with two opposite resistive extensometers (Schenck), inside the furnace. Dog-bone tensile specimens were used, with a length of 200 mm and a thickness between 2 and 5 mm, and a width in the gauge length between 8 and 16 mm. Temperature was measured both with two W–Re 5/26% thermocouples for tests performed in argon (or Pt–Rh 0/10% in air) and an optical pyrometer IRCON Mirage (Niles, USA). SiC–MLAS and SiC_f–YMAS specimens were tensile creep tested with an Instron 1380 machine (Bucks, England), with cold grips. The heating elements in that case were halogen radiant lamps giving the possibility of reaching the desired stabilized temperature in less than 15 min. Displacement was measured with a capacitive extensometer (Instron 3118-230). Specimen size was $150 \times 10\text{--}8 \times 2.5 \text{ mm}^3$. Tests were carried out in air between 1173 and 1373 K. SiC_f–MLAS was also investigated in three point bending under vacuum, between 1273 and 1473 K, on small specimens $14\text{--}30 \times 5 \times 2.5 \text{ mm}^3$ on TiC rods located on tungsten push rods. The machine used was also an Instron 1380 equipped with an opening furnace (Sesame, VMDI, Paris) and tantalum heating elements. The specimen displacement was measured by two LVDT transducers (Penny and Giles, Christchurch, England) attached to the cross-head.

All these tests have been performed with very accurate creep devices. Particular care has been taken especially regarding the load frame alignment, the thermal gradient and its stability, the temperature and strain measurements and the pressure variation inside the furnace.^{32–34} For example most often tests were performed in air-conditioning room, the temperature cartography gave on 22 mm in length a variation of temperature in argon environment less than 7 degrees at 1673 K, and the bending component for the tensile tests was less than 1%. If comparison of creep behavior have to be made, it absolutely requires that creep tests must be performed in conditions as accurate as possible.

SEM observations were performed with a Jeol 6400 (Jeol, Tokyo, Japan), and TEM and HREM with a Jeol 2010 and a Topcon EM 002B (Tokyo, Japan), both equipped with EDS analysis.

Aphelion software (ADCIS, Caen, France) was used to perform automatic image analysis on optical and SEM images, using more specifically the mathematical morphology.^{35,36}

3. Results

We shall first describe the creep macroscopic approach, i.e. the direct results obtained from the creep tests.

3.1. Macroscopic approach

Some strain–time curves, ε – t , (creep curves) are presented in Fig. 2 for different types of CMCs tested in air and in argon. To be sure of the presence of a steady state creep, one plots the creep rate as a function of strain or time, $\dot{\varepsilon}$ – ε or t . The existence of a plateau is a way to confirm a true stationary stage. For each CMCs, two different cases have been evidenced: a primary and a stationary or pseudo-stationary stage. An example is presented in Fig. 3.

At this stage of investigation and in our experimental domain, from these curves one can only say that: the plots are not too noisy, there are two creep stages and no tertiary stage, this class of materials presents a good creep resistance (between 10^{-8} and 10^{-9} s^{-1}) in a domain where un-protected superalloys cannot be used, the fiber woven architecture plays an important role, for example for SiC_f–SiBC the deformation after 20 h at 1473 K under 120 MPa is 3 times that at 1373 K, the total deformation begins to be more important from 1350 K (Fig. 4), and the profit to use Hi-Nicalon fibers compared to NLM 202 is 50 K or 50 MPa at 1473 K. Moreover if one plots the creep rate as a function of temperature, $\dot{\varepsilon}$ – T , an important evolution is observed at temperatures higher than 1450–1475 K (Fig. 5).

To determine a creep mechanism requires other analyses and observations.³⁷

3.2. Creep-mechanism indicator

The observations of the surfaces of the CMC crept specimens by optical and/or scanning electron microscopies, and even by transmission electron microscopy, reveal many types of damage: fiber/matrix debonding, matrix microcracking, yarn/yarn debonding, fiber and yarn bridging, fiber pull-out, fiber rupture, ... (Fig. 6). In fact it corresponds typically to well known energy dissipative mechanisms which enable non-linear stress–strain behavior and have been investigated from a semi-empirical/theoretical approach by many authors in order to accede to some specific parameters which can highlight the micromechanism(s) at work.^{38–44} Such damage has been observed in the case of many other types of CMCs, such as other types of SiC_f–SiC, or SiC_f–Si₃N₄, SiC_f–C, SiC_f–AlO₃, SiC_f–mullite, Al₂O₃–SiC, ..., whatever was the mechanical solicitation (static, tension, compression, bending, creep, fatigue, ...).^{45–55}

In the case of ceramic matrix composites with a glass-ceramic matrix, same types of damage are observed, whatever the matrix is: LAS, CAS, BMAS, MLAS, YMAS.^{21–23,56–59} In the case of bending creep tests, if the specimen is too small, one observes first, and mainly, shear cracks. Maupas analyzed in detail the

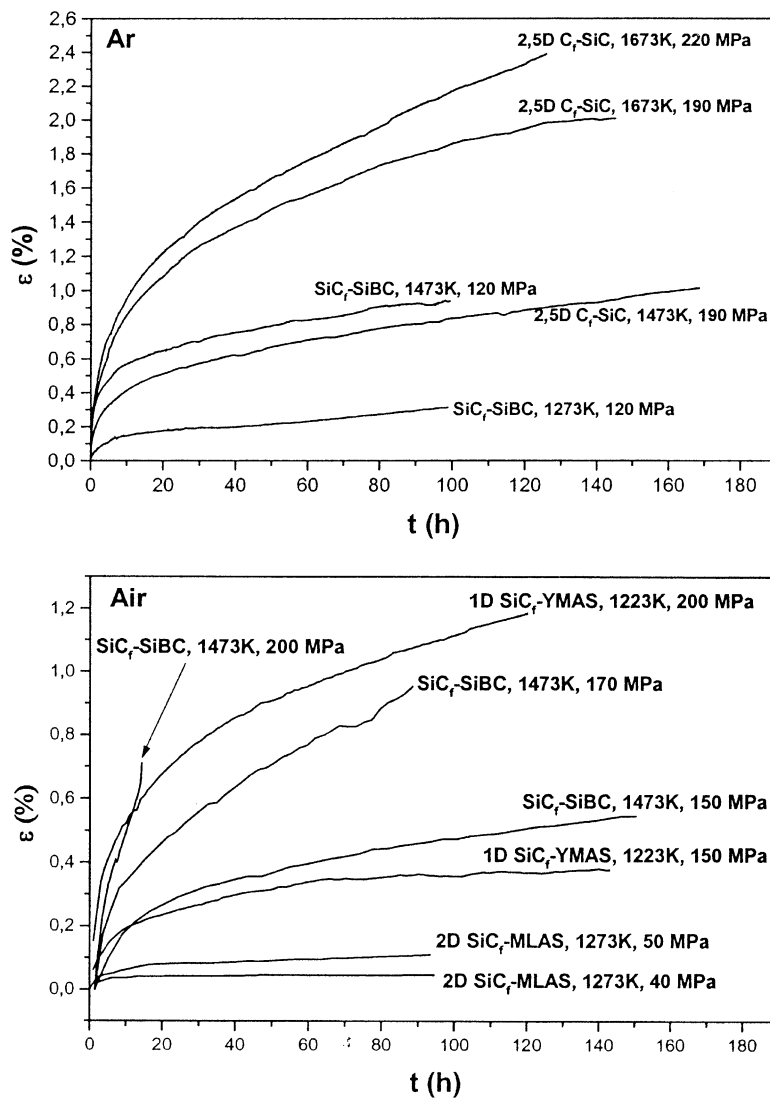


Fig. 2. Strain-time curves, ϵ - t , for different CMCs tensile creep tested at different temperatures and stresses, in argon and air.

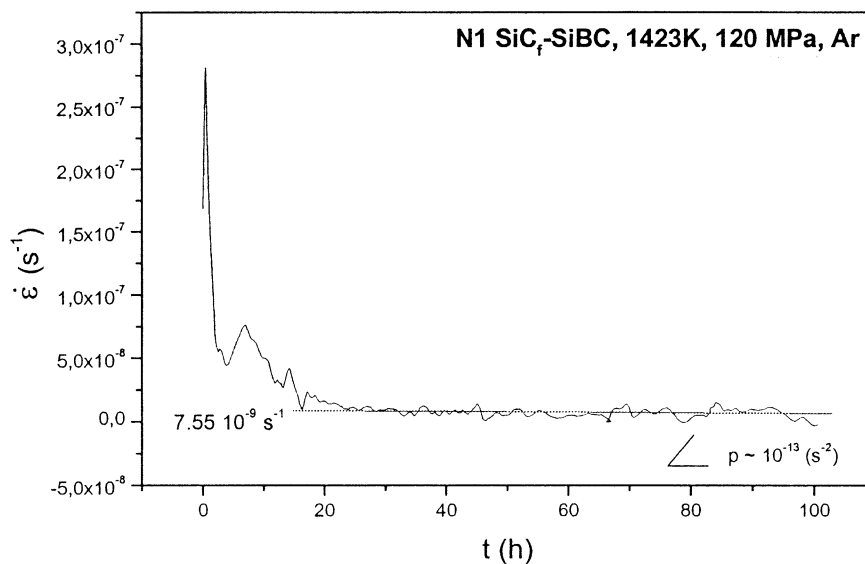


Fig. 3. Strain rate-time, $\dot{\epsilon}$ - t , curve for N1 SiC_r-SiBC tested at 120 MPa under 1423 K: evidence of a stationary stage.

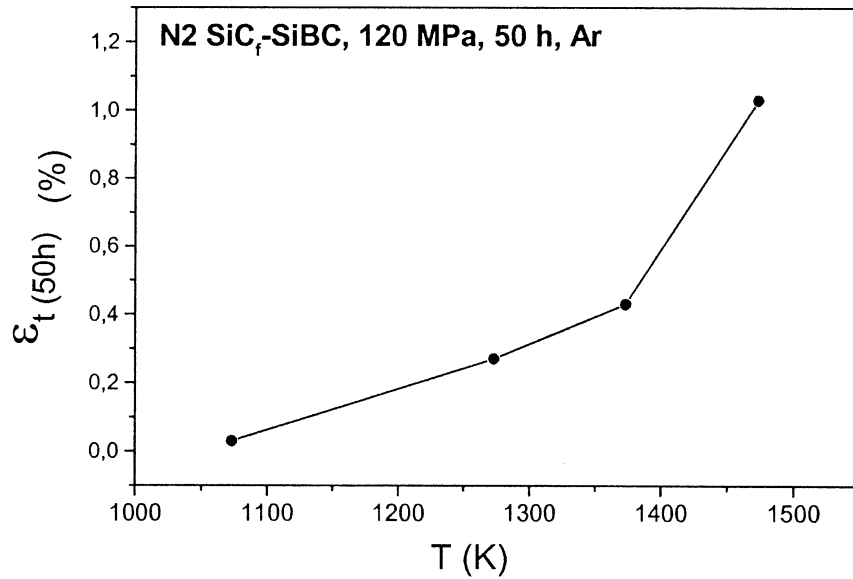


Fig. 4. Variation of the total strain after 50 h of tensile creep as a function of the temperature T , $\epsilon_{t,50}-T$, during a cumulated test in temperatures (1073–1573 K) for N2 SiC_f-SiBC tested at 120 MPa in argon.

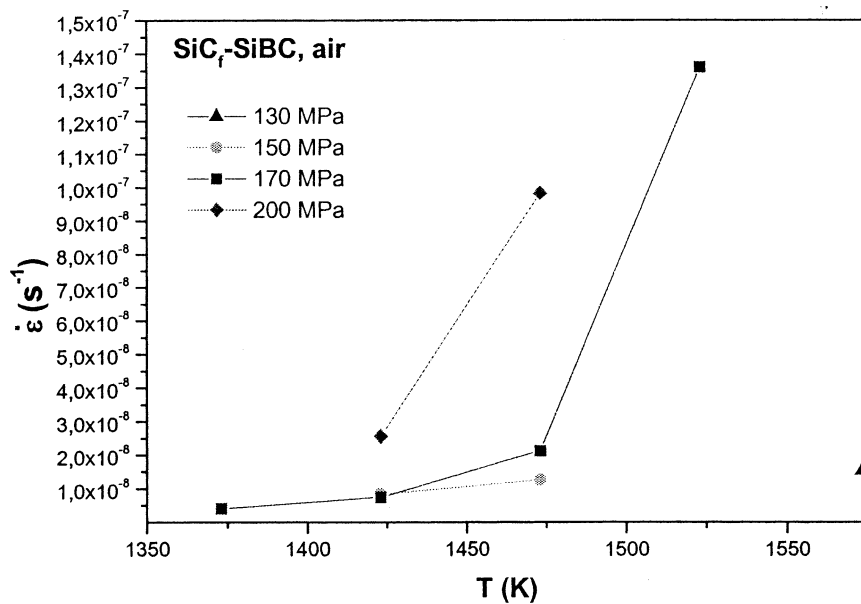


Fig. 5. Change in the creep rate as a function of temperature, $\dot{\epsilon}-T$, for SiC_f-SiBC tensile creep tested in air, at different stresses.

damage development under stress in the case of (0–90°)₆ SiC_f-MLAS composites.^{22,57,58} The damage begins always in the middle 90° ply (Fig. 7a), and then only in the other 90° plies starting from the middle ply. The general crack extension in the 90° plies is controlled by the 0° plies when the applied stress is lower than 200 MPa and the cracks issuing from the 90° plies never cross the 0° plies (Fig. 7b). If the applied stress is higher

than 200 MPa, then the 0° plies start to be damaged by microcracks coming from the 90° plies (Fig. 7c) and then it leads to the rupture of the specimen.

Now if these composites with a glass-ceramic matrix are tested in air, from 1273 K there are always reactions between the SiC fibers and the oxygen to form silica which appears like a glue: it corresponds to the well known oxidative degradation (Fig. 8).

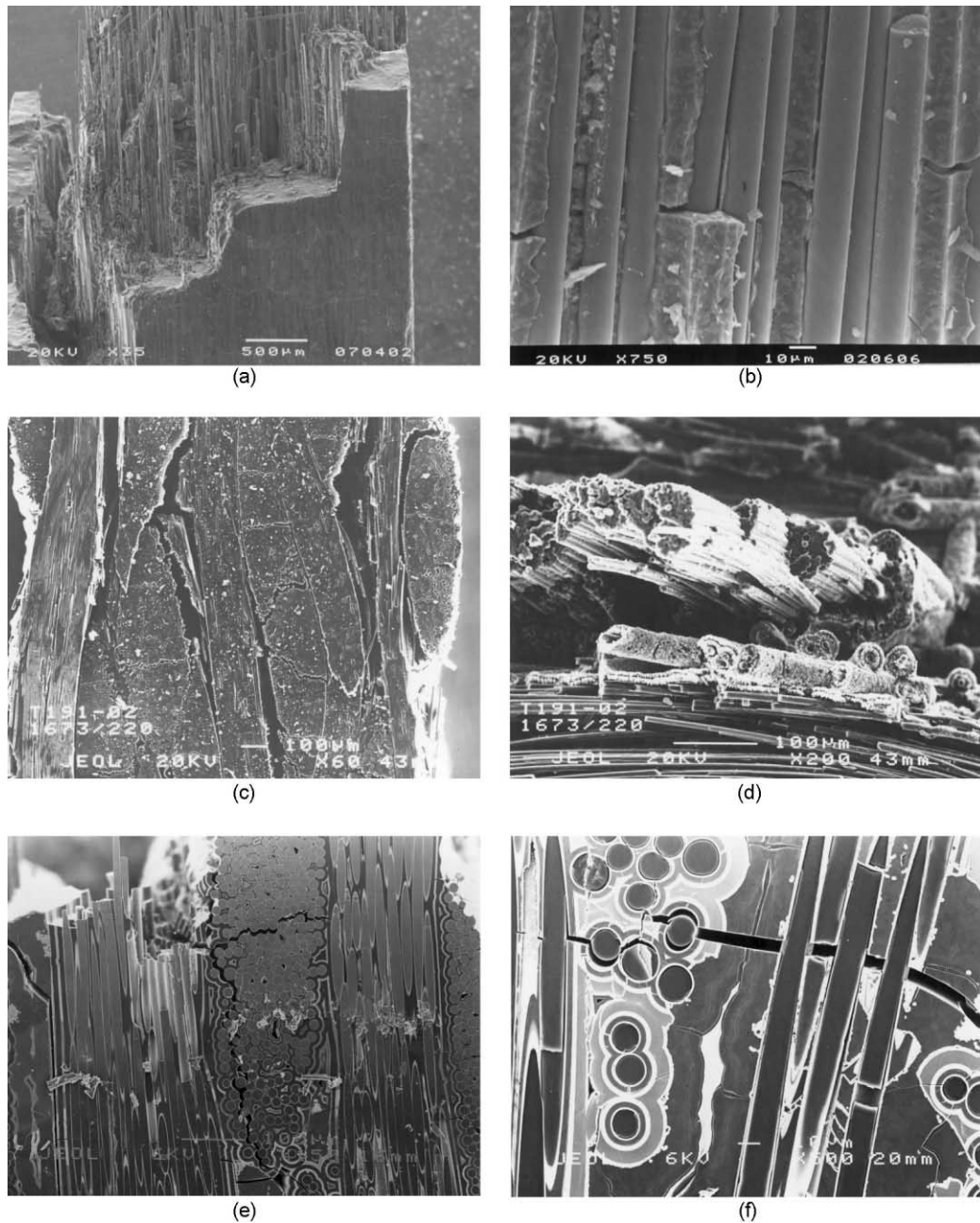


Fig. 6. SEM micrographs of the damages in different CMCs creep tested in Ar or air, at different temperatures and stresses: (a) SiC_f-YMAS, 1223 K, 75 MPa, air; (b) SiC_f-YMAS, 1223 K, 100 MPa, air; (c) C_f-SiC, 1673 K, 220 MPa, Ar; (d) C_f-SiC, 1673 K, 220 MPa, Ar; (e) N1 SiC_f-SiBC, 1473 K, 120 MPa, Ar; (f) N1 SiC_f-SiBC, 1473 K, Ar.

In the case of CMCs with a self-sealing matrix, if tests are performed in air at temperature lower than 1573 K, one observes a crack-healing: the cracks are fullfilled by a glass (Fig. 9a) which prevents oxygen to penetrate further into the microcracks. It is a way, and the reason for the development of these complex multilayered CMCs, to prevent the oxygen to attack the pyrocarbon interphase and the fibers themselves, as is the case for more (and old) classical CMCs (Fig. 9b). Fiber weakening

due to fiber oxidation can be treated like stress corrosion cracking⁵⁹ for Nicalon fibers.

The observations of these crept specimens at higher scales, by TEM and HREM, also reveals the damage but at the microscopic and nanoscopic scales. Fig. 10 presents three examples corresponding to matrix microcrack propagation between some specific matrix layers, a mode I → mode II matrix microcrack deviation and the bridging of a matrix microcrack by nanometric

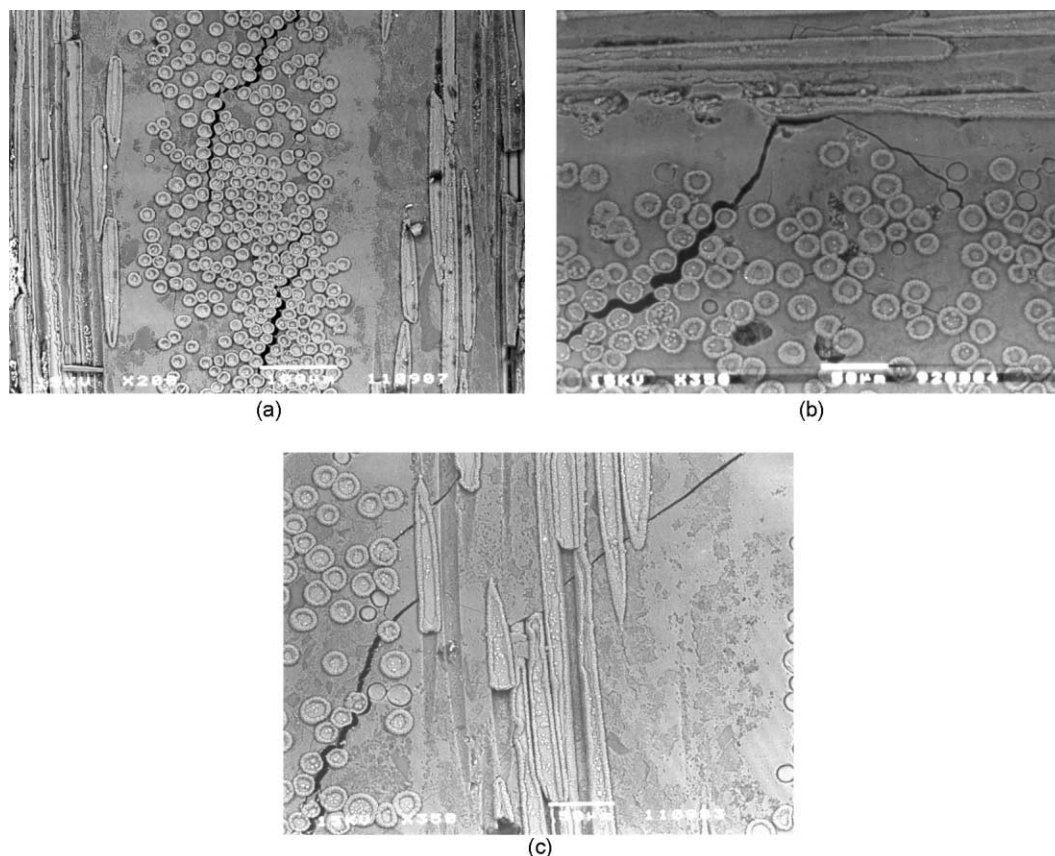


Fig. 7. Micrographs of $(0-90^\circ)_6$ SiC_f -MLAS specimens creep tested in bending at 1373 K, under 200 MPa, in vacuum: (a) microcrack in the 90° ply located in the middle of the specimen; (b) matrix microcrack in a 90° ply; (c) matrix microcracks in 90 and 0° plies.

carbon ribbons. Moreover it is often observed in high resolution lenticular pores in the pyrocarbon, generally parallel to the loading direction: it corresponds, in fact, to the nucleation of the matrix microcracks. Accurate and fine observations and analyses at the nanometric scale show an evolution of the microstructure of the fibers: in the case of SiC_f fibers one observes usually the growth of SiC nanocrystals,^{25,27,60} while in carbon fibers there is an increase of the basic structural units (BSU) and the local molecular orientations (LMO) of these BSUs during the creep: that corresponds to the starting point of the creep of the C_f -SiC composites.^{24,61}

So, for these experimental conditions, only phenomena with matrix, interface and fiber fracture are observed. No specific dislocation motions have been evidenced by TEM or HREM. Moreover in this temperature domain no diffusion phenomena of Si, SiC or C can arise, the temperature being too low: if one analyzes the published diffusion data regarding C and SiC, there is diffusion phenomena above 1828 K⁶² for SiC and above 2423 K for C.^{63,64} Therefore no diffusion-creep mechanism can be activated for these experimental conditions.

In case of CMCs with a glass-ceramic matrix, there is no diffusion data, but from 1273 K the matrices begin

to be viscous and then the ceramic fibers control the creep behavior.

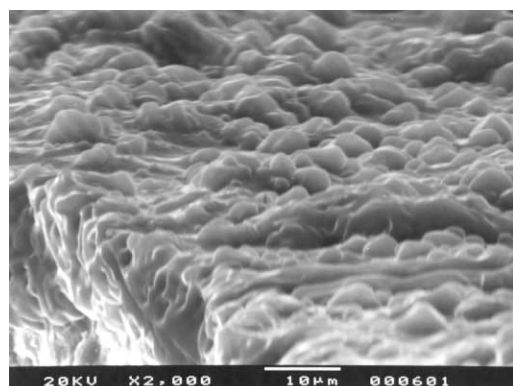
3.3. Damage mechanics approach

The damage mechanics approach proposed by Kachanov⁶⁵ and Rabotnov,⁶⁶ has been adapted to composite materials by Ladevèze.^{67,68} It is in agreement with the fact that many types of damage are observed in these crept materials. In these conditions one has to undertake un-loading and reloading loops during creep tests, in order to follow the change in one of the elastic moduli. The damage parameter, D , is given by:

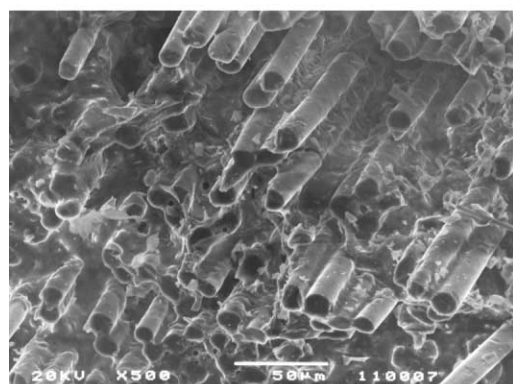
$$D = 1 - \frac{E}{E_0}$$

with: E_0 , the elastic modulus of the un-damaged material; E , the elastic modulus of the damage material at time t (secant modulus of the hysteresis loops).

The plot of the damage parameter, D , as a function of the inelastic strain, ε_{in} , or of time, t , is very instructive (Fig. 11).^{24,26,27,69–71} The same type of curves has been obtained for C_f -SiC, SiC_f -SiC, SiC_f -SiBC tensile creep tested in argon, and also in air. Two stages



(a)



(b)

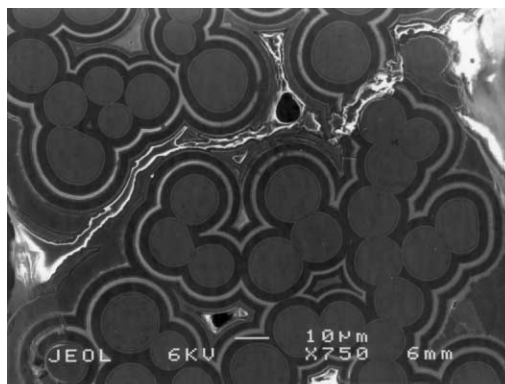
Fig. 8. SEM micrographs of two CMCs with a glass-ceramic matrix creep tested in tension, in air: (a) surface of a 1D SiCf-YMAS, after 50 h of creep at 1223 K under 75 MPa; (b) (0–90°)₆ SiCf-MLAS, after 25 h of creep at 1373 K under 60 MPa.

are evidenced: (1) a very rapid increase of the damage at the beginning or during the loading; (2) a second stage which evolves very slowly. These two stages have to be now explained.

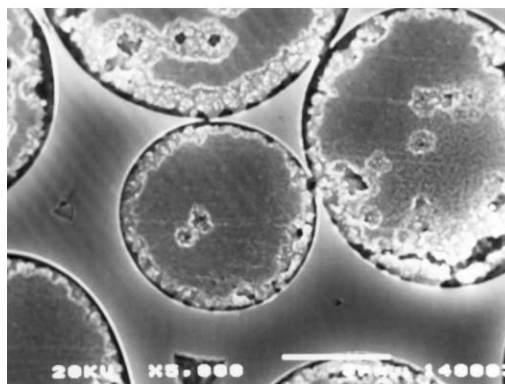
The damage parameter appears not only as a fruitful tool for monitoring damage evolution in these materials, but it also can be used to model the creep curves from an extension of the isotropic damage macro-model proposed initially by Ladevèze,^{67,68} applied to high temperature tests with the introduction of a visco-plastic potential,⁷² (Fig. 12).

4. Discussion

Since no dislocation creep⁷³ or diffusion creep^{74–76} are involved in the case of CMCs creep tested at low stress and low temperature, one considers at the LERMAT that the so-called damage creep mechanism^{77,78} controls the creep deformation of these materials. This is based on the results of the damage mechanics, on the observations at the different scales, and on some results using other techniques.



(a)



(b)

Fig. 9. Influence of the oxidation on CMCs: (a) crack healing in a SiCf-SiBC specimen tensile creep tested at 1473 K under 170 MPa, in air; (b) first step of the oxidation of the pyrocarbon layer in a 2D SiCf-SiC specimen bending creep tested at 1573 K under 200 MPa and in vacuum.

For example in the case of C_f-SiC or SiC_f-SiC composites tensile creep tested in argon, respectively Boitier²⁴ and Darzens²⁷ have shown that there is creation of matrix microcracks and from a certain time an opening of the transverse matrix microcracks with the development of longitudinal matrix microcracks mainly between the yarns (Fig. 13). That opening is intensified at constant temperature by the stress (the opening increases with stress) or, to a lower extent, at constant stress by the temperature, and no new matrix microcracks are observed.

Boitier^{24,79,80} and Darzens^{27,80} have used automatic image analysis to quantify these damages. For C_f-SiC composites, the surface fractions of matrix microcracks increases from 1.4 (for the as-received material) to 6.4 (for a material tensile creep tested at 1673 K, at 200 MPa, in Ar, during 130 h) and the surface area of the yarns increases respectively from 135 650 to 146 900 µm². So a swelling of the specimens is observed and has been quantified. For N1 and N2 SiC_f-SiBC composites, the matrix microcrack opening, e_m , has been quantified and related to the inelastic deformation, ϵ_{in} , after tensile creep tests at 1473 K under 120 MPa and in argon. A

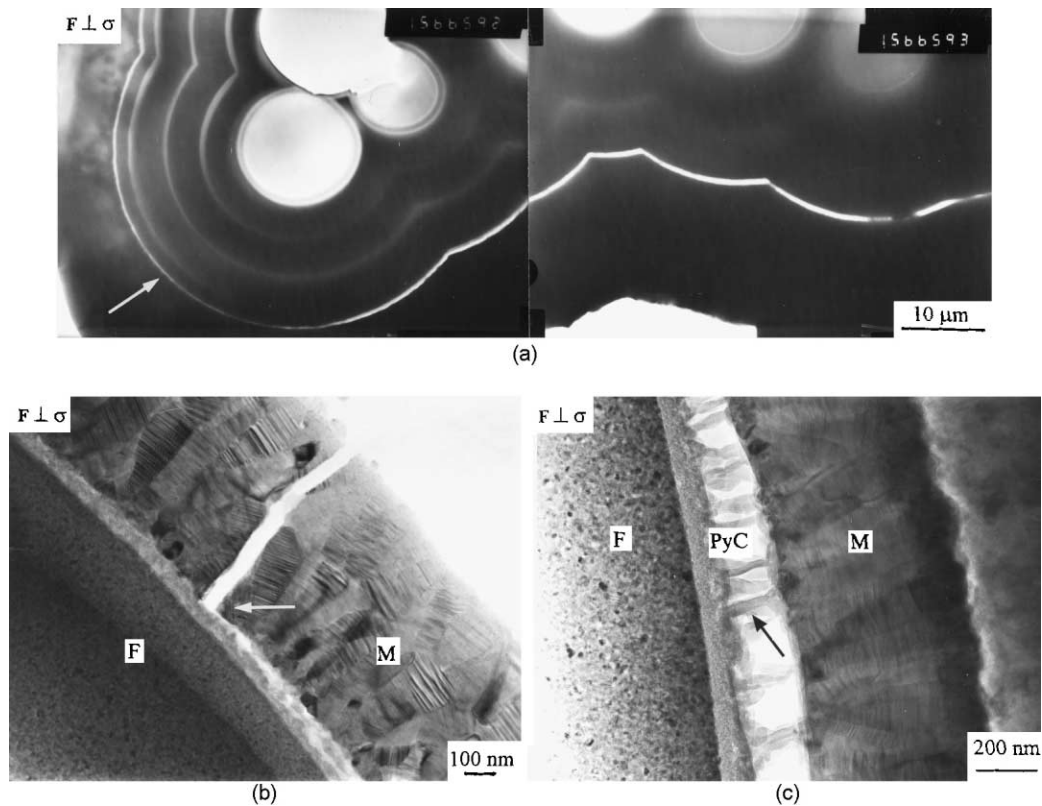


Fig. 10. TEM micrographs showing in the case of $\text{SiC}_f\text{-SiBC}$ specimens tensile creep tested in Ar: (a) matrix microcrack between matrix layers (1473 K, 200 MPa); (b) mode I \rightarrow mode II deviation (1523 K, 120 MPa); (c) carbon nanofilaments bridging a microcrack (1473 K, 200 MPa).

linear relationship is obtained (Fig. 14). It appears that for N2 composites the microcrack opening evolves more largely than for N1 composites, while the microcrack interdistance remains similar: 650 and 610 μm , respectively for N1 and N2 composites. This difference informs on the existence of two different damage mechanisms which confirms the macroscopical and damage mechanics results. Darzens²⁷ has shown that the carbon interface is not the same and then it leads to different microcrack process.

From all these results one can propose a creep mechanism in two stages, which is plausible. First there is creation and development ($\text{SiC}_f\text{-SiC}$, $\text{SiC}_f\text{-SiBC}$) or development ($\text{C}_f\text{-SiC}$) of a matrix microcrack pattern until its saturation. In the case of $\text{SiC}_f\text{-SiBC}$ and $\text{C}_f\text{-SiC}$ that microcracking array is formed very rapidly during the loading and, probably, a little thereafter. The microcracks grow through the transverse yarns, by passing the fibers. In the case of SiC_f fibers, the matrix microcracks are generally nucleated at the inter-yarns macropores, as it has been shown, for example by Guillaumat and Lamon.⁸¹ That damage corresponds to the first part of the $D\text{-}\varepsilon_{\text{in}}$ or $D\text{-}t$ curves (Fig. 11). At this stage the load is mainly carried by the longitudinal yarns. In the case of $\text{C}_f\text{-SiC}$, Boitier^{24,82} has clearly shown that five types of matrix microcracks are developed according

to the direction of the fiber architecture with regard to the loading direction (Fig. 15). Inter-yarn cracks are typically resulting from the straightening of the longitudinal yarns parallel to the loading direction, as it has previously been described by Schuler et al.⁸³ Secondly, after the matrix microcrack saturation, the propagation in the longitudinal yarns and opening of the microcracks in the transverse yarns have been shown both from microscopic observations and from the measurement of the opening of the matrix transverse microcracks by means of automatic image analysis:^{79,80} it corresponds to the second part of the curve. Then some of the matrix microcracks become master (dominant) cracks and one of these leads to the rupture of the specimen.^{24,27,82} That last rupture mechanism can be assimilated to a slow crack growth process, SCG, well known for glass and ceramic materials.^{84,85}

The straightening of the longitudinal yarns parallel to the loading direction appears as one of the driving forces for the damage development, and consequently for the creep of such composites. That straightening induces bending efforts in the transverse yarns and the subsequent “V-like” (or “flexural type”) opening of the transverse microcracks and the appearance of longitudinal cracks (type [4] in Fig. 15) in the transverse yarns.⁸³ That was confirmed also by some in-situ

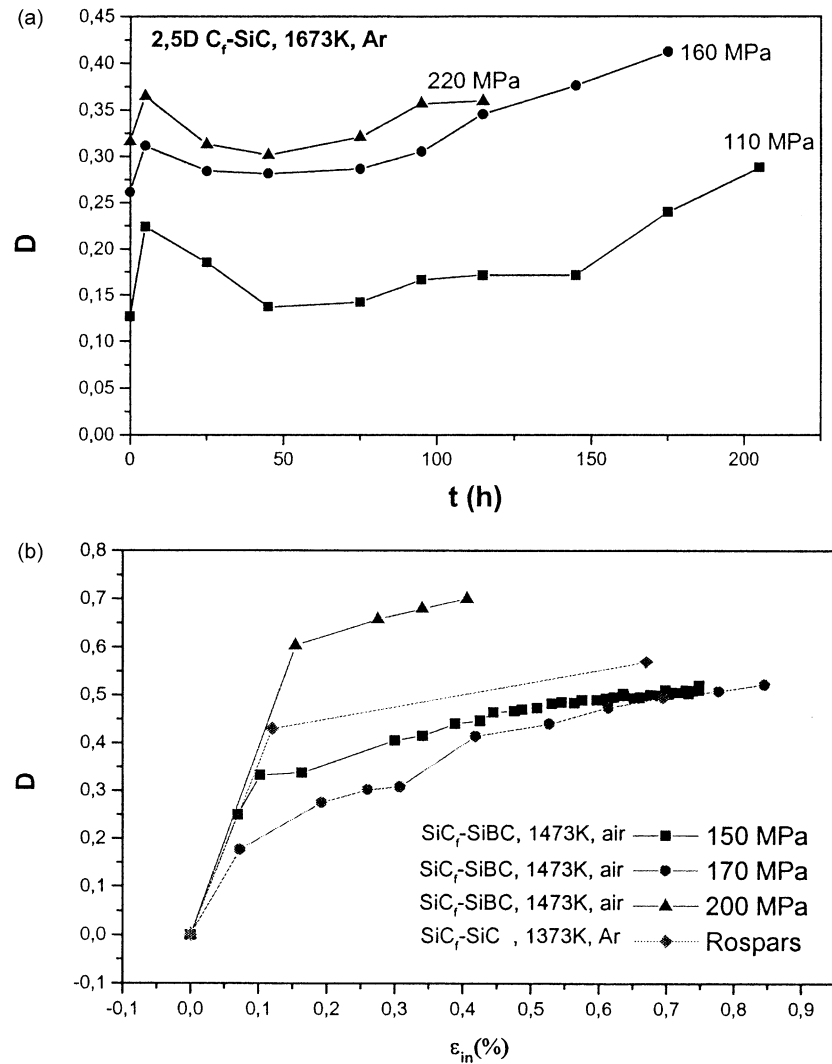


Fig. 11. Evolution of the damage parameter, D , as a function of: (a) time, t , for C_f -SiC specimens tensile creep tested at 1673 K in Ar; (b) inelastic deformation, ϵ_{in} , for SiC_f-SiC and SiC_f-SiBC specimens tensile creep tested at 1473 K respectively in Ar (results from Rospars²⁶ at 110, 125 and 130 MPa) and air.

experiments carried out at room temperature on polished 2D C_f -SiC specimens: one observes the opening of these cracks under load, but at rupture they close up (Fig. 16).^{86,87}

Finally in the case of CMC based on SiC fibers, when the longitudinal matrix microcracks are bridged by some SiC_f fibers, their creep can operate. At 1473 K Darzens²⁷ has shown for tensile creep of SiC_f-SiBC under argon that the strain follows a logarithmic evolution during the pseudo-stationary stage at 1473 K, while at 1373 and 1423 K it is a linear one, both for N1 and N2 composites. Consequently the creep strain of N1 and N2 composites can be governed by a relationship as:

$$\epsilon = a \left(\frac{t}{t_0} \right)^b$$

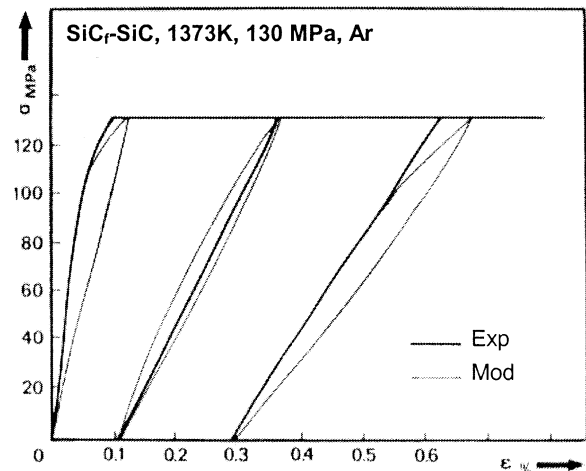


Fig. 12. Comparison of experimental (Exp.) and model (Mod.) curves for 2D SiC_f-SiC specimen creep tested in tension at 1373 K at 130 MPa in argon, with unloading-reloading loops performed during the creep test to access to the damage parameter. From Rospars.²⁶

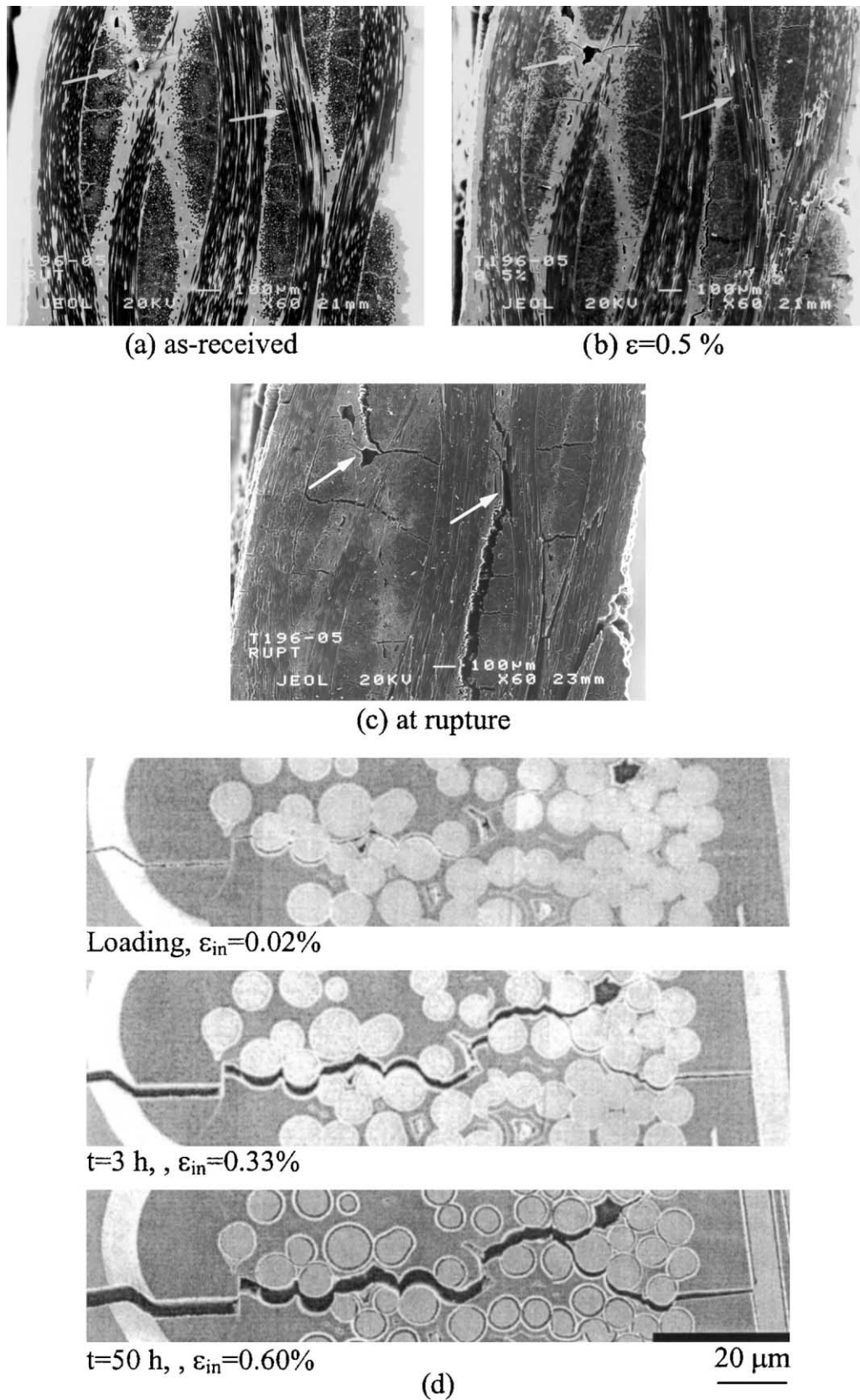


Fig. 13. Matrix microcrack evolution: for C_f-SiC, tensile creep tested at 1673 K in Ar, at 220 MPa for different strain, ϵ : (a) as received; (b) $\epsilon=0.5\%$; (c) at rupture; (d) for N₂ SiC_f-SiBC (transverse microcrack), during tensile creep tests at 1473 K, at 120 MPa, in Ar, after different creep time, t , (1, 3 and 50 h).

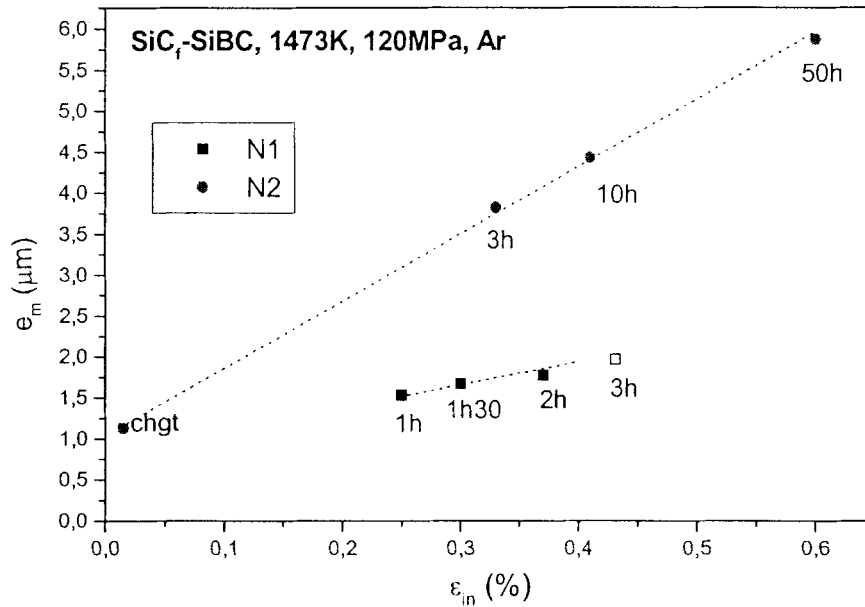


Fig. 14. Change in the microcrack opening, e_m , as a function of the inelastic strain, ϵ_{in} , for N1 and N2 SiC_f -SiBC specimens, tensile creep tested at 1473 K and 120 MPa, in air, for different creep times (in h).

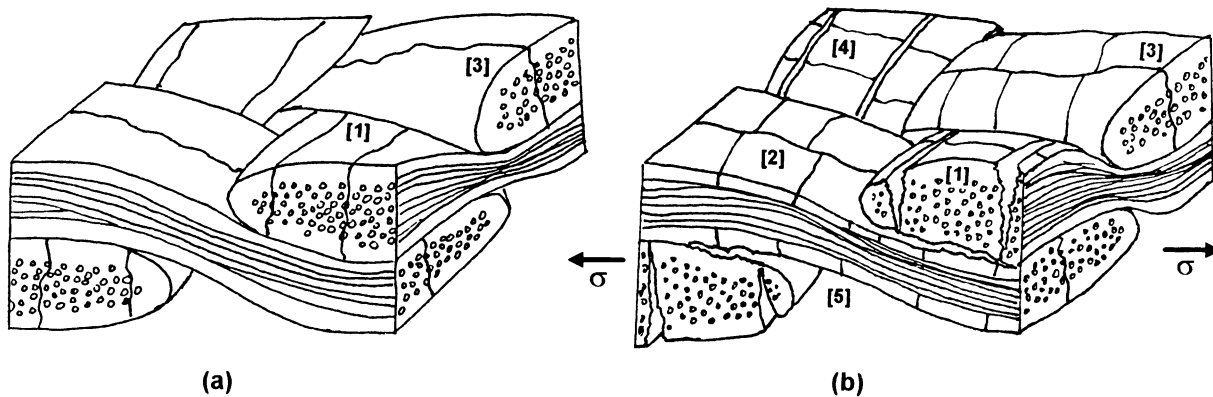


Fig. 15. Schematic illustration of the five types of matrix microcracks in a C_f -SiC composite: (a) as received; (b) after tensile creep test.

with a , the strain at t_0 (%); b , the time exponent; t_0 , the reference time, taken in these experiments as 1 h.

Fig. 17 presents some creep curves for N2 SiC_f -SiBC specimens, tensile creep tested at 1473 K under 120 MPa, and the corresponding power law plots. The values of b are between 0.19 and 0.24. Carrère⁸⁸ during his work on the same type of composite has observed a similar evolution. If one takes the creep results of the Nicalon NLM 202 under argon by Bodet,⁸⁹ Carrère has shown that at the same temperature, but under 450 MPa, these SiC_f fibers follow a similar power law with the same exponent. This logarithmic evolution for the strain has also been observed by several authors for the Nicalon fibers.^{90–92} So one concludes that the creep behavior of SiC_f -SiBC of type N is controlled by the creep of the Nicalon fibers, while for type H (Hi-Nicalon) composites the fiber creep is not activated at 1473

K, under 120–150 MPa: only a linear deformation in the stationary stage is observed and the creep is controlled by the longitudinal yarns.²⁷ In these conditions the crack growth is limited by the crack bridging of the SiC_f fibers. In the case of tensile tests performed in air, one observes an oxidation-assisted fiber rupture due to the oxygen penetration, which has to be investigated and quantified.⁹³ These results are in agreement with the deformation and damage processes proposed by Wilshire and Carreño for SiC_f -SiC and SiC_f - Al_2O_3 .⁹⁴

Our observations and analysis demonstrate that the matrix microcracking control the rates of strain accumulation in these materials, with a stress transfer from the matrix to the fibers, and a possible creep of the SiC fibers which accompagnies the matrix microcracking depending on the experimental temperature and stress conditions. So from all these results one can propose for

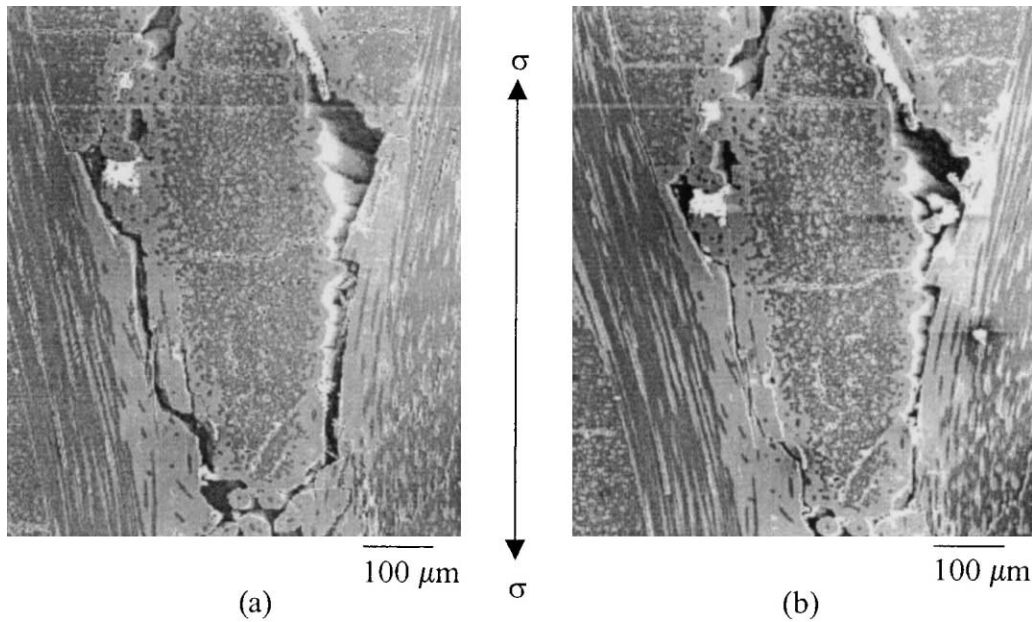


Fig. 16. 2D SiC_f-SiC specimen during an in-situ tensile test at room temperature in a SEM: (a) development of an inter-yarn crack under a load of 1500 N; (b) same area at rupture (1550 N): one notes the inter-yarn crack closing.

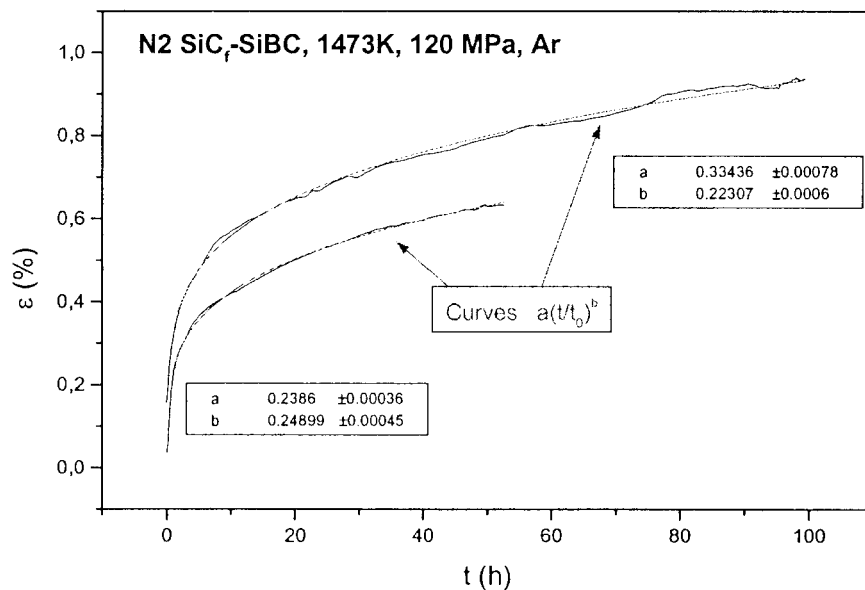


Fig. 17. Creep curves and corresponding power law for N2 SiC_f-SiBC specimen tensile creep tested at 1473 K, in argon, at 120 MPa.

these CMCs with a ceramic matrix, the schematic mechanism of Fig. 18, with the possibility of creep for the ceramic fibers under specific conditions of load and strain: first we have the matrix microcracking in the transverse yarns (Fig. 18b) and in the longitudinal yarns until their saturation (Fig. 18c), accompanied by fiber/matrix and yarn/yarn debonding; so there is a reloading on the fibers, mainly longitudinal, giving the possibility to the SiC fibers bridging the matrix microcracks to creep and which is facilitated by the crack openings

(Fig. 18d and e); one of the main matrix crack becomes the master crack, leading to the rupture of the longitudinal yarns, which is made easier by the fiber/matrix and yarn/yarn debondings. Such mechanism approached by material science concepts seems also to agree with the different published results on CMCs, as those already quoted or those concerning a more general overview or a comparison of creep results^{94–96} although, as written previously, it is very difficult to compare published results from different laboratories, as the

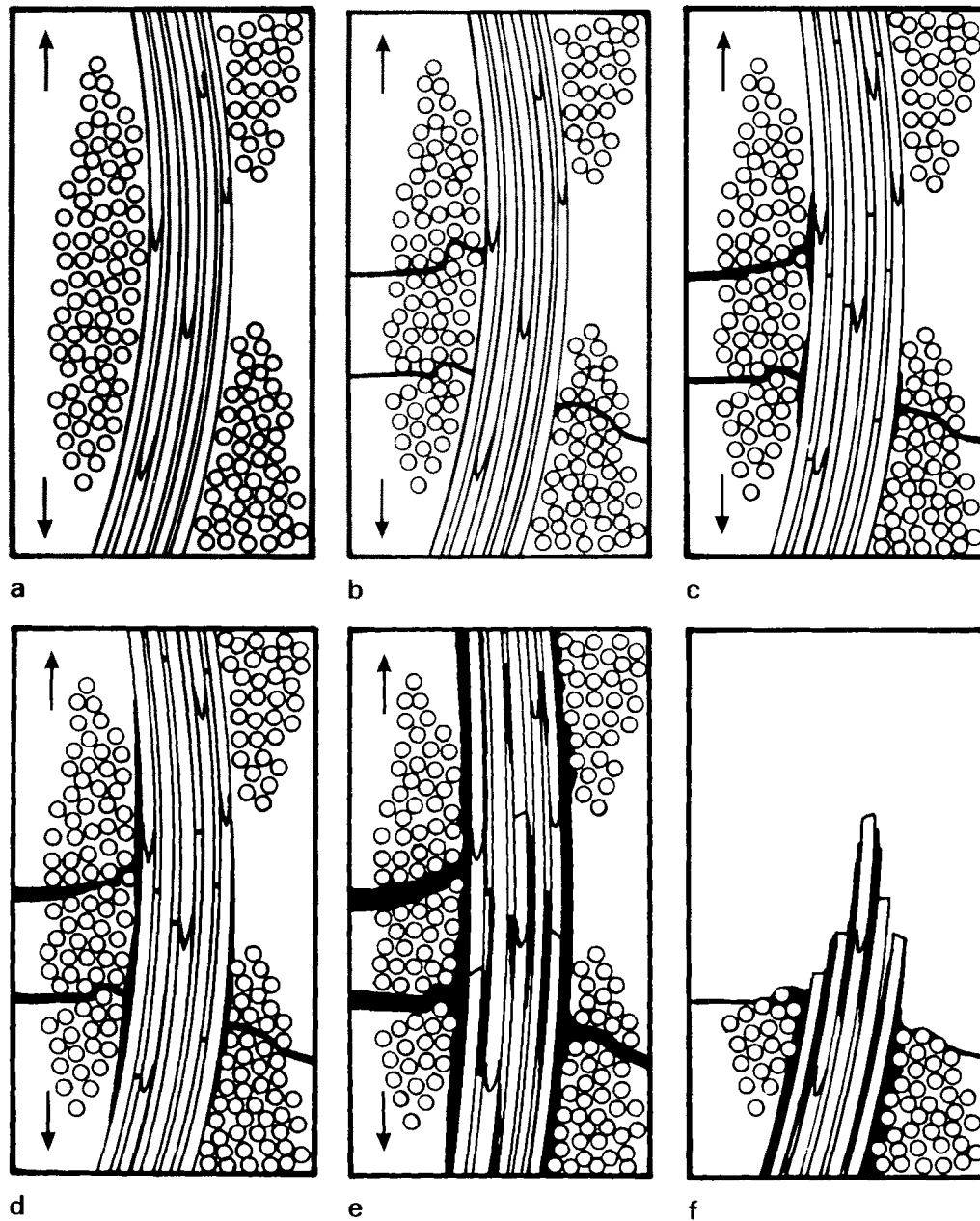


Fig. 18. Schematic illustration of the tensile creep in CMCs. These sequences are based on true micrographs of the observed damages (arrows indicate the loading direction).

experimental conditions and morphologies are most often different. That was also supported by the very recent papers of Henager et al.^{97,98} on crack growth activation energies and time temperature exponents for $\text{SiC}_f\text{-SiC}$ also tested in argon; it agrees with fiber creep activation energies and non-linear creep equations for both SiC_f types: the growth of subcritical cracks in argon for NLM 202 and Hi-Nic fiber reinforced CVI silicon carbide matrices is controlled by fiber creep processes. A dynamic crack growth model has also been developed by these authors⁹⁸ to predict the slow crack growth in ceramic matrix composites containing non-linear, creeping fibers in an elastic matrix.

5. Conclusion

This paper has resumed more than 10 years of research at LERMAT on the creep of several batches of CMCs with a ceramic or glass-ceramic matrix and the role of the microstructure. It has shown that the creep of ceramic matrix composites reinforced by continuous ceramic fibers with a ceramic matrix is controlled by a damage creep mechanism, while for those with a glass-ceramic matrix above 1273 K it is controlled by the fibers. For the first class the creep mechanism is in two stages: first a matrix microcracking until its saturation, followed by an opening of the transverse microcracks

occurring with the inter-yarn debonding and the micro-crack development in the matrix of longitudinal yarns. When the ceramic fibers bridge the longitudinal matrix cracks, if conditions of temperature and stress are adequate (high enough) the SiC fibers can creep, but not the carbon fibers in our experimental domain investigated. Such results are the consequence of multiscale and multitechnique investigations, which are absolutely necessary to understand the mechanical behavior of such complex materials.

One has also shown that damage mechanics is a suitable tool to describe the mechanical behavior of these materials and that automatic image analysis permits to quantify the damages and to bring to the mechanical engineers morphological parameters of the damages, which have now to be included in the damage mechanics formalisms. Such approach also enables to correctly model the creep curves,^{72,99,100} without any hypothesis on the different components: fibers, matrix, fiber/matrix interfaces. That is a very positive point. Other models to describe the creep behavior are also proposed based either on damage-enhanced creep, fiber damage, time-dependent failure by fiber degradation or interface shear creep, creep-crack growth with small bridging or a bridging law for creeping fibers, or even on finite element methods based on simulations of the mechanical response of composites.^{101–107}

These CMCs based on ceramic matrices appear as very good creep resistant materials in a field where classical and un-protected alloys or superalloys cannot be used. Moreover thermal barrier coatings (TBC) are developed and modelled today to still improve all these types of composites.^{108–113}

Acknowledgements

This work has been supported by SEP, now SNECMA Propulsion Solide (St Médard en Jalles, France) and by CNRS and Région of Basse-Normandie (GB, SD, GF). This study was partially performed in the frame of the research program CPR-DV “Contrat Programme de Recherche: Modélisation du comportement et de la longévité de composite à matrice céramique—Modelling of the behavior and life time of ceramic matrix composites”, with ENS-Cachan, GEMPPM-Villeurbanne, LCTS-Pessac, LERMAT-Caen, ONERA-Châtillon sous Bagneux, and SNECMA Propulsion Solide-St Médard en Jalles. We wish to warmly thank Drs. F. Abbé, F. Doreau, D. Kervadec, H. Maupas and C. Rospars for some of their creep results on the creep of some CMCs investigated in our Laboratory, Drs. M. Bourgeon, E. Pestourie and J.M. Rougès for fruitful discussions and for providing the specimens, Mrs. L. Chermant for the morphological investigations by automatic image analysis, and Mr. H.

Cubero for his helpful assistance to perform creep tests in the “best” conditions.

References

1. Lamicq, P., The break through of thermostructural composites. In *Science et Défense 90, Nouvelles Avancées Scientifiques et Techniques*. Dunod, Paris, 1990, pp. 80–92.
2. Lamicq, P. and Jamet, J. F., Thermostructural CMCs: an overview of the French experience. In *High Temperature Ceramic-Matrix Composites I, HT-CMC I*, vol. 57, *Ceram. Trans.*, ed. A. G. Evans and R. Naslain, 1995, pp. 1–11.
3. Fohey, W. R., Battison, J. M. and Nielsen, T. A., Ceramic composite turbine engine component evaluation. *Ceram. Eng. Sci. Proc.*, 1995, **16**, 459–466.
4. Shirouzu, M. and Yamamoto, M., Overview of the HYFLEX project. *Am. Inst. Aeron. Astronautics*, 1996, **4524**, 1–8.
5. Spriet, P. and Habarou, G., Applications of continuous fiber reinforced ceramic composites in military turbojet engines. *Key Eng. Mat.*, 1997, **132–136**, 1930–1933.
6. Beesley, C. P., The application of CMCs in high integrity gas turbine engines. *Key Eng. Mat.*, 1997, **127–131**, 165–174.
7. Brockmeyer, J. W., Ceramic matrix composite applications in advanced liquid fuel rocket engine turbomachinery. *J. Eng. Gas Turbines & Power, Trans. ASME*, 1999, **115**, 58–63.
8. Imuta, M. and Gotoh J., Development of high temperature materials including CMCs for space application. In *High Temperature Ceramic Matrix Composites, HT-CMC III*, Osaka, Japan, 6–9 September, 1998, ed. by K. Niihara, K. Nakano, T. Sekino and E. Yasuda, CSJ Series, *Ceram. Soc. Jap.*, 1999, **3**, 439–444.
9. Nishio, K., Igashira, K. I., Take, K. and Suemitsu, T., Development of a combustor liner composed of ceramic matrix composite, CMC. *J. Eng. Gas Turbines & Power, Trans. ASME*, 1999, **121**, 12–17.
10. Ohnabe, H., Masaki, S., Onozuka, M., Miyahara, K. and Sasa, T., Potential application of ceramic matrix composites to aero-engine components. *Composites Part A*, 1999, **30A**, 489–496.
11. Trabandt, U., Wulz, H.G. and Schmid, T., CMC for hot structures and control surfaces of future launchers. In *High Temperature Ceramic Matrix Composites, HT-CMC III*, Osaka, Japan, Sep. 6–9, 1998, ed. by K. Niihara, K. Nakano, T. Sekino and E. Yasuda, CSJ Series, *Ceram. Soc. Jap.*, 1999, **3**, 445–450.
12. Jones, R. H. and Henager, C. H., High temperature properties of SiC/SiC for fusion applications. *J. Nucl. Mater.*, 1994, **212–215**, 830–834.
13. Staehler, J. M. and Zavada, L. P., Performance of four ceramic-matrix composite divergent flap inserts following ground testing on an F 110 turbofan engine. *J. Am. Ceram. Soc.*, 2000, **83**, 1727–1738.
14. Medvedovski, E., High-alumina armor ceramic tile for ballistic protection. *Am. Ceram. Soc. Bull.*, 2001, **80**, 25.
15. Labbé, P., Les freins d'Airbus sur nos voitures ? Bientôt ! *C.E.A. Technologies*, 1998, **40**, 8.
16. Bensimhon, V., Les matériaux composites dans le groupe SNECMA. *AMACINFOS*, 1999, **11**, 1–2.
17. Renz R. and Krenkel W., C/C-SiC composites for high performance emergency brake systems. In *Composites: from Fundamentals to Exploitation, ECCM 9*, 4–7 June 2000, Brighton, UK, ECCM 9 CD ROM C 2000, IOM Communications Ltd.
18. Gadow, R. and Speicher, M., Manufacturing and CMC-component development for brake disks in automatic applications. *Ceram. Eng. Sci. Proc.*, 1999, **20**, 551–558.
19. Naslain, R., Fibre matrix interphases and interfaces in ceramic matrix composites processed by CVI. *Comp. Interfaces*, 1993, **1**, 253–286.

20. Tressler, R. E., Recent developments in fibers and interphases for high temperature ceramic matrix composites. *Composites, Part A*, 1999, **A30**, 429–437.
21. Kervadec, D., *Comportement en fluage sous flexion et microstructure d'un SiC_f-MLAS 1D*. Thèse de Doctorat of the University of Caen, 1992.
22. Maupas, H., *Fluage d'un composite SiC_f-MLAS 2D en flexion et en traction*. Thèse de Doctorat of the University of Caen, 1996.
23. Doreau, F., *Microstructure, morphologie et comportement en fluage de composites SiC_f-YMAS unidirectionnels*. Thèse de Doctorat of the University of Caen, 1995.
24. Boitier, G., *Comportement en fluage et microstructure de composites C_f-SiC 2,5D*. Thèse de Doctorat of the University of Caen, 1997.
25. Abbé, F., *Fluage en flexion d'un composite SiC_f-SiC 2D*. Thèse de Doctorat of the University of Caen, 1990.
26. Rospars, C., *Modélisation du comportement thermomécanique de composites à matrice céramique : étude du SiC_f-SiC 2D en fluage*. Thèse de Doctorat of the University of Caen, 1997.
27. Darzens, S., *Fluage en traction sous argon et microstructure de composites SiC_f-SiBC*. Thèse de Doctorat of the University of Caen, Dec. 2000.
28. Farizy, G., *Mécanisme de fluage de composites céramiques SiC_f-SiBC à matrice autocicatrisante*, Thèse de Doctorat of the University of Caen. To be defended in 2002.
29. Christin, F., Naslain, R. and Bernard, C., A thermodynamic and experimental approach of silicon carbide CVD. Application to the CVD-infiltration of porous carbon-carbon composites. In *Proceedings of the 7th International Conference on CVD*, ed. T. O. Sedwick and H. Lydtin. The Electrochemical Society, Princeton, 1979, pp. 499–514.
30. Goujard, S. and Vandenbulcke, L., Deposition of Si-B-C materials from the vapor phase for applications in ceramic matrix composites. *Ceram. Trans.*, 1994, **46**, 925–935.
31. Darzens, S., Vicens, J. and Chermant, J. L., Microstructure and morphology of SiC_f-SiBC composites. *Eur. Phys. J. Appl. Phys.*, 2001, **15**, 35–48.
32. Boitier, G., Maupas, H., Cubero, H. and Chermant, J. L., Sur les essais de traction à longs termes à haute température. *Rev. Comp. Mat. Avancés*, 1997, **7**, 143–172.
33. Jenkins, M. G., Wiederhorn, S. M. and Shiffer, R. K., *Creep Testing of Advanced Ceramics*. Marcel Dekker, New-York, 1998.
34. Boitier, G., Cubero, H. and Chermant, J.L., Some recommendations for long term high temperature tests. In *High Temperature Ceramic Matrix Composites, HT-CMCIII*, CSJ Series, *Ceram. Soc. Japan*, 1999, **3**, 309–312.
35. Serra, J., *Mathematical Morphology and Image Analysis*. Academic Press, New-York, 1982.
36. Coster, M. and Chermant, J.L., *Précis d'Analyse d'Images*, Les Editions du CNRS, Paris, 1985; 2nd edn., Les Presses du CNRS, Paris, 1989.
37. Boitier, G., Chermant, J. L. and Vicens, J., Multiscale investigation of the creep behavior of a 2.5D C_f-SiC composites. *J. Mater. Sci.*, 1999, **34**, 2759–2767.
38. Budiansky, B., Hutchinson, J. W. and Evans, A. G., Matrix fracture in fiber-reinforced ceramics. *J. Mech. Phys. Solids*, 1986, **34**, 167–189.
39. Thouless, M. D., Sbaizero, O., Sigl, L. S. and Evans, A. G., Effect of interface mechanical properties on pull-out in a SiC fiber reinforced lithium aluminium silicate glass-ceramic. *J. Am. Ceram. Soc.*, 1989, **72**, 525–532.
40. Spearing, S. M. and Evans, A. G., The role of fiber bridging in the delamination resistance of fiber-reinforced composites. *Acta Metall. Mater.*, 1992, **40**, 2192–2199.
41. Curtin, W. A., Toughening of crack bridging in heterogeneous ceramic. *J. Am. Ceram. Soc.*, 1995, **18**, 1313–1323.
42. He, M. Y., Wissuchek, D. J. and Evans, A. G., Toughening and strengthening by inclined ligament bridging. *Acta Mater.*, 1997, **45**, 2813–2820.
43. Okabe, T., Takeda, N., Komotori, J., Shimizu, M. and Curtin, W. A., A new fracture mechanics model for multiple matrix cracks of SiC fiber reinforced brittle-matrix composites. *Acta Mater.*, 1999, **47**, 4299–4309.
44. Boitier, G., Chermant, J. L. and Vicens, J., Bridging at the nano-metric scale in 2.5D C_f-SiC composites. *Appl. Comp. Mater.*, 1999, **6**, 279–287.
45. Adami, J.N., *Comportement en fluage uniaxial sous vide d'un composite à matrice céramique bidirectionnel Al₂O₃-SiC*. Thèse de Doctorat ès Science Techniques, Ecole Polytechnique Fédérale de Zürich (Switzerland), prepared at the Institut for Advanced Materials, Commission of the European Communities, Petten, The Netherlands, 1992.
46. Adami, J.N., Bressers, J. and Steen, M., Creep behaviour of a 2D Al₂O₃-SiC ceramic composite under vacuum. In *Proceedings of the Conference on Materials 91*, Lisbon, Portugal, 1991, vol. 2, pp. 571–583.
47. Holmes, J. W., Tensile creep behaviour of a fiber-reinforced SiC-Si₃N₄ composite. *J. Mater. Sci.*, 1991, **26**, 1808–1814.
48. Mozdierz, N. and Backhaus-Ricoult, M., High temperature creep performance and microstructure of SiC-C-SiC composites. *J. Phys. IV*, 1993, **C7**, 1931–1936.
49. Weber, C. H., Kim, K. T., Heredia, F. E. and Evans, A. G., High temperature deformation and rupture in SiC-C composites. *Mater. Sci. Eng.*, 1995, **A196**, 25–31.
50. Dalmaz, A., Reynaud, P., Rouby, D. and Fantozzi, G., Damage propagation in carbon/silicon carbide composites during tensile tests under the SEM. *J. Mater. Sci.*, 1996, **31**, 4213–4219.
51. Wilshire, B. and Carreño, F., Deformation and failure processes during tensile creep of fibre and whisker reinforced SiC/Al₂O₃ composites. *Mater. Sci. Eng.*, 1999, **A272**, 38–44.
52. Zawada, L., Butkus, M. and Hartman, G. A., Tensile and fatigue behavior of silicon carbide fiber-reinforced aluminosilicate glass. *J. Am. Ceram. Soc.*, 1991, **74**, 2851–2858.
53. Wu, X. and Holmes, J. W., Tensile creep and creep strain recovery behavior of silicon carbide fiber calcium aluminosilicate matrix ceramic composites. *J. Am. Ceram. Soc.*, 1993, **76**, 2695–2700.
54. Weber, C. H., Löfvander, J. P. A. and Evans, A. G., Creep anisotropy of a continuous fiber-reinforced silicon carbide calcium aluminosilicate composite. *J. Am. Ceram. Soc.*, 1994, **77**, 1745–1752.
55. Beyerlee, D. S., Spearing, S. M. and Evans, A. G., Damage mechanisms and the mechanical properties of a laminated 0/90 ceramic matrix composite. *J. Am. Ceram. Soc.*, 1992, **75**, 3321–3330.
56. Sun, E. Y., Nutt, S. R. and Brennan, J. J., Flexural creep of coated SiC-fiber-reinforced glass-ceramic composites. *J. Am. Ceram. Soc.*, 1995, **78**, 1233–1239.
57. Maupas, H., Kervadec, D. and Chermant, J. L., Damage creep in SiC_f-MLAS composites. In *Fracture Mechanics of Ceramics, FMC 6, vol. 12*, ed. R. C. Bradt, D. P. H. Hasselman, D. Munz, M. Sakai and V. Y. Shevchenko. Plenum Press, NY, 1996, pp. 527–538.
58. Maupas, H., Rospars, C. and Chermant, J.L., Crack growth in the 90° plies and creep of 2D SiC_f-MLAS composites. In *Proceedings of the 1st International Conference on Ceramic and Metal Matrix Composites, CMMC 96*, San-Sebastian, Spain, 9–12 September, 1996, ed. by M. Fuentes, J.M. Martinez-Esnaola and A.M. Daniel, Trans. Tech. Pub., *Key Eng. Mat.*, 1997, **127–131**, pp 769–776.
59. Evans, A. G., Zok, F. W., Mc Meeking, R. M. and Du, Z. Z., Models of high-temperature, environmentally assisted embrittlement in ceramic-matrix composites. *J. Am. Ceram. Soc.*, 1996, **79**, 2345–2352.

60. Le Coustumer, P., Monthieux, M. and Oberlin, A., Understanding Nicalon fibre. *J. Eur. Ceram. Soc.*, 1993, **11**, 95–103.
61. Boitier, G., Vicens, J. and Chermant, J. L., Carbon fiber nano-creep in creep-tested C_f-SiC composites. *Scripta Mater.*, 1998, **38**, 937–943.
62. Carter, C. H., Davis, R. F. and Bentley, J., Kinetics and mechanisms of high-temperature creep in silicon carbide chemically vapor deposited. *J. Am. Ceram. Soc.*, 1984, **67**, 732–740.
63. Sines, G., Yang, Z. and Vickers, B. D., Creep of carbon yarn and a carbon-carbon composite at high temperature and high stresses. *Carbon*, 1989, **27**, 403–415.
64. Kogure, K., Sines, G. and Lavin, J. G., Structural studies of post-creep, Pan-based, carbon filaments. *Carbon*, 1994, **32**, 715–726.
65. Kachanov, L., Rupture time under creep conditions. *Izv. Akad. Nauk. SSR*, 1958, **8**, 26–31.
66. Rabotnov, M., *Creep Problem in Structural Members*. North Holland, Amsterdam, 1969.
67. Ladevèze, P., *Sur une théorie de l'endommagement anisotrope (Internal Report no. 34)*. Laboratoire de Mécanique et de Technologie de Cachan, France, 1983.
68. Ladevèze, P., On an anisotropic damage theory. In *Failure Criteria of Structured Media*, ed. J. P. Boehler. Balkema, Rotterdam, 1993, pp. 355–363.
69. Darzens, S., Farizy, G., Vicens, J., Chermant, J.L. and Sangleboeuf, J.C., Multiscale investigation in the creep behavior of SiC_f-SiBC. In *4th High Temperature Ceramic Matrix Composite Conference, HT-CMC IV*, Munchen, Germany, 1–3 October 2001, ed. W. Krenkel, R. Naslain and H. Schneider. Wiley-VCH, Weinheim, Germany, 2001, pp. 211–217.
70. Chermant, J. L. and Boitier, G., The importance of damage and slow crack growth in the creep behavior of ceramic matrix composites. *Adv. Comp. Mater.*, 1999, **8**, 77–85.
71. Boitier, G., Chermant, J. L. and Vicens, J., Understanding the creep behavior of a 2.5D C_f-SiC composite: II Experimental specifications and macroscopical mechanical creep response. *Mater. Sci. Eng.*, 2000, **A289**, 265–275.
72. Rospars, C., Chermant, J. L. and Ladevèze, P., On a first creep model for a 2D SiC_f-SiC composite. *Mater. Sci. Eng.*, 1998, **A250**, 264–269.
73. Poirier, J. P., *Creep of Crystals: High-Temperature Deformation Processes in Metals Ceramics and Minerals*. Cambridge University Press, Cambridge, 1985.
74. Nabarro, F.R.N., Deformation of crystals by the motion of single ions. In *Report of a Conference on Strength of Solids*, The Physical Society, Bristol, England 1948, pp. 75–90.
75. Herring, C., Diffusional viscosity of a polycrystalline solid. *J. Appl. Phys.*, 1950, **21**, 437–445.
76. Coble, L., A model for boundary-diffusion controlled creep in polycrystalline materials. *J. Appl. Phys.*, 1963, **34**, 1679–1682.
77. Kervadec, D. and Chermant, J. L., Some aspects of the morphology and creep behavior of a SiC_f-MLAS material. In *Fracture Mechanics of Ceramics, FMC 5, vol. 10*, ed. R. C. Bradt, D. P. H. Hasselman, D. Munz, M. Sakai and V. Y. Shevchenko. Plenum Press, New York, 1992, pp. 459–471.
78. Chermant, J. L., Creep behavior of ceramic matrix composites. *Sil. Ind.*, 1995, **60**, 261–273.
79. Boitier, G., Chermant, L. and Chermant, J. L., Morphological characterization of carbon-silicon carbide composites. *Acta Stereol.*, 1997, **16**, 275–280.
80. Boitier, G., Darzens, S., Chermant, L., Coster, M. and Chermant, J. L., Damage quantification of CMCs by image analysis. In *High Temperature Ceramic Matrix Composite, HT-CMC IV*, Munchen, Germany, 1–3 October, 2001, ed. W. Krenkel, R. Naslain and H. Schneider. Wiley-VCH, Weinheim, Germany, 2001, pp. 557–563.
81. Guillaumat, L. and Lamon, J., Multifissuration de composites SiC-SiC. In *Microstructure, Comportements Thermomécaniques et Modélisation de Composites Céramique-Céramique à Fibres*. Special issue ed. by J.L. Chermant and G. Fantozzi. *Rev. Comp. Mater. Avancés*, 1993, **3HS**, 159–171.
82. Boitier, G., Vicens, J. and Chermant, J. L., Understanding the creep behavior of a 2.5D C_f-SiC composite. III. From mesoscale to nanoscale microstructural and morphological investigations towards creep mechanism. *Mater. Sci. Eng.*, 2001, **A313**, 56–63.
83. Shuler, S. F., Holmes, J. W., Wu, X. and Roach, D., Influence of loading frequency on the room-temperature of a carbon-fiber/SiC-matrix composite. *J. Am. Ceram. Soc.*, 1993, **76**, 2327–2336.
84. Evans, A. G. and Wiederhorn, S. M., Proof testing of ceramic materials-an analytical basis for failure prediction. *Int. J. Fract.*, 1974, **10**, 379–392.
85. Evans, A. G., A method for evaluating the time-dependent failure characteristics of brittle materials-and its application to polycrystalline alumina. *J. Mater. Sci.*, 1972, **7**, 1137–1146.
86. Delanoë, A. and Fauchoux, V., *Etude de l'endommagement de CMC par des expériences de traction in-situ*. Project of 3rd year at ENSI-ISMRA, Caen, 2001.
87. Chermant, J.L., 2001 (in preparation).
88. Carrère, P., *Comportement thermomécanique d'un composite de type SiC/SiC*. Thèse de Doctorat of the University of Bordeaux I, 1996.
89. Bodet, R., *Comportement à la rupture à chaud et en fluage, évolution microstructurale de fibres issues de précurseurs organosiliciés*. Thèse de Doctorat of the University of Bordeaux I, 1993.
90. Bodet, R., Lamon, J. and Tressler, R., Effects of chemical environments on the creep behavior of SiCO fibers. In *High Temperature Ceramic Matrix Composites I, HT-CMC1*, ed. by R. Naslain, J. Lamon and D. Doumeingts, Woodhead, 1993, pp. 75–83.
91. Tressler, R. and DiCarlo J., High temperature mechanical properties of advanced ceramic fibers. In *High Temperature Ceramic Matrix Composites I, HT-CMC1*, ed. by R. Naslain, J. Lamon and D. Doumeingts, Woodhead, 1993, pp. 33–39.
92. DiCarlo, J. and Yun, H., Creep and rupture behaviour of advanced fibers. In *ICCM-10*, Vancouver, British Columbia, Canada, 1995, pp. 315–322.
93. Viricelle, J. P., Goursat, P. and Bahloul-Hourlier, D., Oxidation behaviour of a multi-layered ceramic-matrix composite (SiC)_f/C/SiBC_m. *Comp. Sci. Tech.*, 2000, **61**, 607–614.
94. Wilshire, B. and Carreño, F., Deformation and damage processes during tensile creep of ceramic-fibre-reinforced ceramic-matrix composites. *J. Eur. Ceram. Soc.*, 2000, **20**, 463–472.
95. Fantozzi, G., Chevalier, J., Olagnon, C. & Chermant, J.L., Creep of ceramic matrix composites. In *Encyclopedia of Materials: Science and Technology: vol 4: Carbon/Carbon, Cement and Ceramic Matrix Composites*, ed by K.H.J. Buschow, R.W. Cahn, M.C. Flemings, B. Illschner, E.J. Kramer and S. Mahajan. Elsevier Science, 2000, Vol. 4, ch 9, pp. 115–162.
96. Wilshire, B., Creep property comparisons for ceramic-fibre-reinforced ceramic-matrix composites. *J. Eur. Ceram. Soc.* (in press).
97. Henager, C. H., Lewinsohn, C. A. and Jones, R. H., Subcritical crack growth in CVI SiC_f/SiC composites at elevated temperatures: effect of fiber creep rate. *Acta Mater.*, 2001, **49**, 3727–3738.
98. Henager, C. H. and Hoagland, R. G., Subcritical crack growth in CVI SiC_f/SiC composites at elevated temperatures: dynamic crack growth model. *Acta Mater.*, 2001, **49**, 3739–3753.
99. Rospars, C., Le Dantec, E. and Lecuyer, F., A micromechanical model for thermostructural composites. *Comp. Sci. Tech.*, 2000, **60**, 1095–1102.
100. Ladevèze, P., Letombe, S. and Cluzel, C., A CMCs damage model based on micro and macro-mechanics for high temperature and complex loadings. In *High Temperature Ceramic Matrix Composite, HT-CMC IV*, Munchen, Germany, 1–3 October 2001, ed. W. Krenkel, R. Naslain and H. Schneider. Wiley-VCH, Weinheim, Germany, 2001, pp. 578–583.

101. Sony, Y., Bao, G. and Hui, C. Y., On creep of unidirectional fiber composites with fiber damage. *Acta Metall. Mater.*, 1995, **43**, 2615–2623.
102. Fabeny, B. and Curtin, W. A., Damage-enhanced creep and rupture in fiber-reinforced composites. *Acta Mater.*, 1996, **44**, 3439–3451.
103. Iyengar, N. and Curtin, W. A., Time dependent failure in fiber-reinforced composites by fiber degradation. *Acta Mater.*, 1997, **45**, 1489–1502.
104. Begley, M. R., Cox, B. N. and McMeeking, R. M., Creep crack growth with small scale bridging in ceramic matrix composites. *Acta Mater.*, 1997, **45**, 2897–2909.
105. Iyengar, N. and Curtin, W. A., Time-dependant failure in fiber reinforced composites by matrix and interface shear creep. *Acta Mater.*, 1997, **45**, 3419–3429.
106. Cox, B. N., Sridhar, N. and Argento, C. R., A bridging law for creeping fibres. *Acta Mater.*, 2000, **48**, 4137–4150.
107. Yang, S., Gokhale, A. M. and Shau, Z., Utility of micro-structure modeling for simulation of micro-mechanical response of composites containing non-uniformly distributed fibers. *Acta Mater.*, 2000, **48**, 2307–2322.
108. Webster, J. D., Westwood, M. E., Hayes, F. H., Day, R. J., Taylor, R., Duran, A., Aparicio, M., Rebstock, K. and Vogel, W. D., Oxidation protection coatings for C/SiC based on yttrium silicate. *J. Eur. Ceram. Soc.*, 1998, **18**, 2345–2350.
109. Callender, R. L. and Barron, A. R., Formation of interface coatings on SiC and sapphire fibers using metal doped carboxylate-alumoxanes. *Ceram. Eng. Sci. Proc.*, 1999, **20**, 127–134.
110. Parthasarathy, T. A., Boakye, E. E., Keller, K. A. and Hay, R. S., Evaluation of porous $\text{ZrO}_2\text{-SiO}_2$ and monazite coatings using NextelTM 720-fiber-reinforced BackglasTM mini-composites. *J. Am. Ceram. Soc.*, 2000, **84**, 1526–1532.
111. Ferraris, M., Montorsi, M. and Salve, M., Glass coating for SiC_f/SiC composites for high temperature applications. *Acta Mater.*, 2000, **48**, 4721–4724.
112. Mumm, D. R., Evans, A. G. and Spitsberg, I. T., Characterisation of a cycle displacement instability for a thermally grown oxide in a thermal barrier system. *Acta Mater.*, 2001, **49**, 2329–2340.
113. Karlsson, A. M. and Evans, A. G., A numerical model for the cyclic instability of thermally grown oxides in thermal barrier systems. *Acta Mater.*, 2000, **49**, 1793–1804.